Electronic Supplementary Material (ESI) for Dalton Transactions.

Supporting Information

Single-ion magnet behavior of Ln^{3+} encapsulated in carbon nanotube. An *ab initio* insight

Dan Liu[1]*, Xuefeng Guo[1], Xiaoyong Zhang[2], Abdullah A. Al-Kahtani[3], Liviu F. Chibotaru[4]*

[1]Institute of Flexible Electronics, Northwestern Polytechnical University, 127 West Youyi Road, Xi'an, 710072 Shaanxi, China
[2]Institute of Systems and Physical Biology, Shenzhen Bay Laboratory, Shenzhen 518055, China
[3]Chemistry Department, College of Science, King Saud University, P.O. Box 2455, Riyadh 11451, Saudi Arabia
[4]Theory of Nanomaterials Group, Katholieke Universiteit Leuven, Celestijnenlaan 200F, Leuven B-3001, Belgium

***Ab initio* insight: single ions magnet behavior of Ln^{3+} encapsulated in carbon nanotube**

The diameters of DFT optimized pristine zigzag nanotubes and calculated ones for R_{CC} = 1.4 Å [1] are shown in Table S1. One can see an enlargement of the diameters of all CNTs of ca 0.2 Å upon optimization. The last row in Table S1 gives the diameter of the closest to Tb ring of carbon atoms in the fully optimized embedded CNT Tb^{3+}@(5,0). The corresponding structural model used in ab initio calculations is shown in Fig. 1, while Fig. S1 gives similar structural models for non-optimized and diameter optimized only CNT fragments. These are used for the sake of identification of the role of structural distortions of C atoms surrounding the Ln^{3+} ion in the observed multiplet spectra and magnetic anisotropy of embedded CNTs. The relevant structural distortions can be inferred from Tables S2 and S3.

Table S1. The diameters (Å) of non-optimized, optimized pristine and optimized embedded CNT.

CNTs	**(5,0)**	**(6,0)**	**(7,0)**
Non-optimized	3.91	4.70	5.48
Optimized pristine	4.08	4.84	5.60
Fully optimized (closest C ring to Tb)	4.20	4.94	5.68

(a)

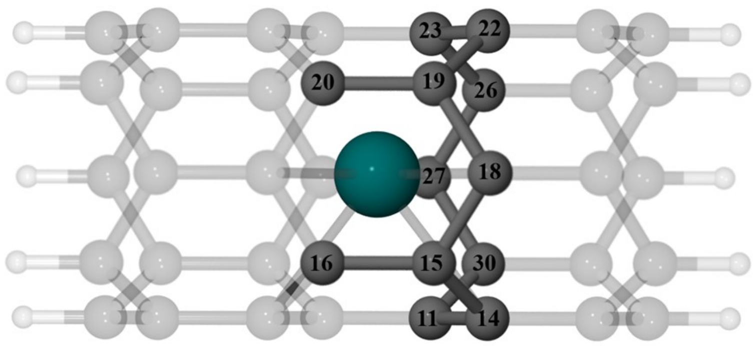

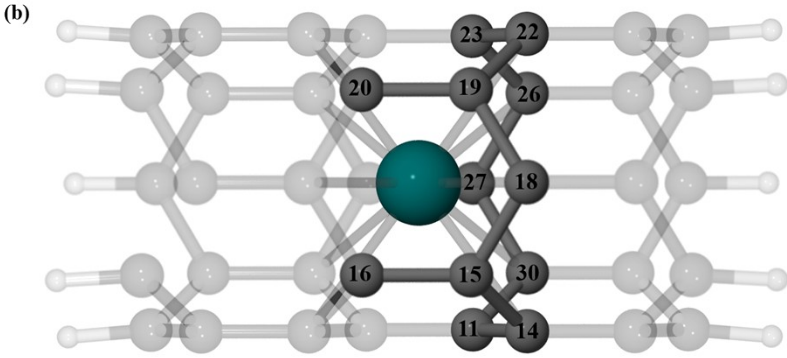

Figure S1. Structural models of Tb^{3+} embedded into (5,0) zigzag CNT with non-optimized (a) and partly optimized (b) nanotubes (see the text). The labelled black balls highlight nearest and next nearest carbon atoms to the Tb^{3+} ion.

Table S2. The distances (Å) between Tb^{3+} ion and the nearest and next nearest C atoms in non-optimized, CNT diameter optimized only and fully optimized (5,0) CNTs.

Tb-C_n		**Non-optimized**	**CNT diameter optimized only**	**Fully optimized**
nearest	Tb-C_{11}	2.1	2.2	2.3
	Tb-C_{15}	2.1	2.2	2.3
	Tb-C_{19}	2.1	2.2	2.3
	Tb-C_{23}	2.1	2.2	2.3
	Tb-C_{27}	2.1	2.2	2.3
next-nearest	Tb-C_{14}	2.4	2.5	2.6
	Tb-C_{18}	2.4	2.5	2.6
	Tb-C_{22}	2.4	2.5	2.6
	Tb-C_{26}	2.4	2.5	2.6
	Tb-C_{30}	2.4	2.5	2.6

Table S3. The angles (°) between nearest C atoms and the Tb^{3+} ion in non-optimized, CNT diameter optimized only and fully optimized (5,0) CNTs.

$<C_{n1}C_nC_{n3}$	**Non-optimized**	**CNT diameter optimized only**	**Fully optimized**
$<C_{15}C_{18}C_{19}$	110.2	111.2	117.6
$<C_{18}C_{19}C_{20}$	120.4	119.8	117.8

$<C_{16}C_{15}C_{18}$	120.4	119.8	117.8

Table S4. The Mulliken charges on Tb^{3+} ion, the nearest and next nearest C atoms in non-optimized, CNT diameter optimized only and fully optimized (5,0) CNTs.

Atoms		**Non-optimized**	**CNT diameter optimized only**	**Fully optimized**
Tb^{3+}		0.96	1.12	1.26
nearest	C_{11}	-0.08	-0.09	-0.05
	C_{15}	-0.09	-0.10	-0.06
	C_{19}	-0.11	-0.11	-0.05
	C_{23}	-0.11	-0.11	-0.06
	C_{27}	-0.09	-0.10	-0.06
next-nearest	C_{14}	0.07	0.05	-0.01
	C_{18}	0.08	0.07	0.00
	C_{22}	0.08	0.07	-0.05
	C_{26}	0.08	0.07	0.02
	C_{30}	0.07	0.06	-0.05

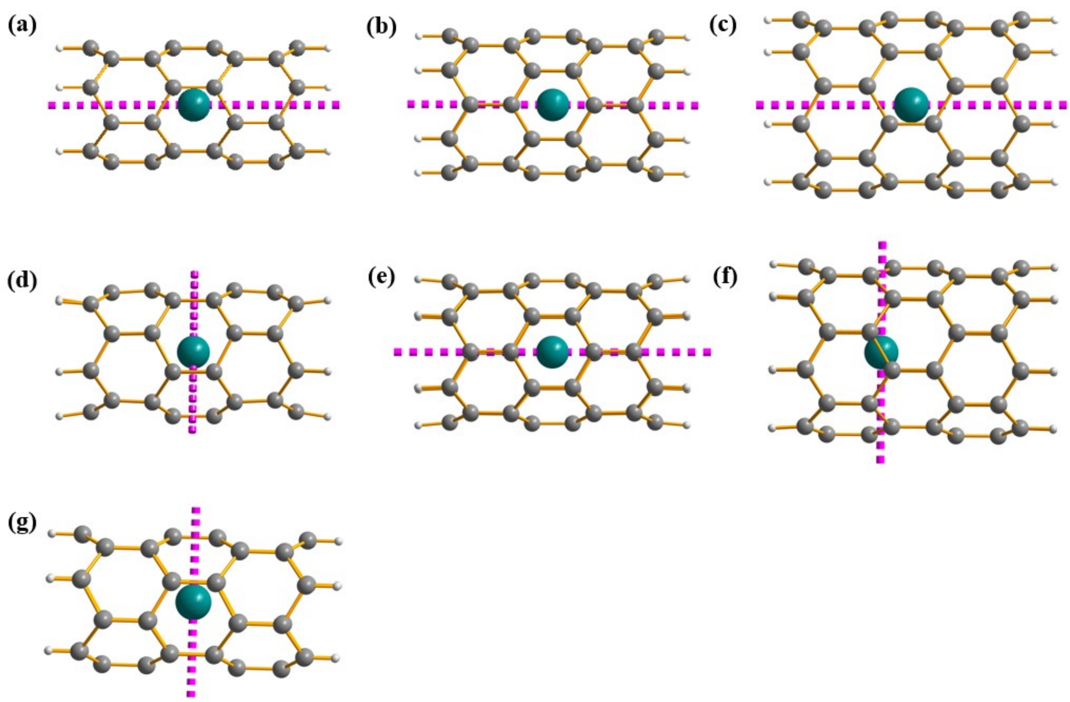

Figure S2. Position of Tb^{3+} in the (5,0), (6,0) and (7,0) CNTs (top row are non-optimized, middle row are fully optimized and bottom is CNT diameter optimized only) and main magnetic axis (pink arrow). Color code: Tb^{3+} (green), H (gray) and C (dark gray).

Table S5. Energies of the lowest doublets (cm^{-1}) of Tb^{3+} in (5,0), (6,0) and (7,0) CNTs (non-optimized) and (5,0) CNT (CNT diameter optimized only).

Spin-orbit energies, cm^{-1}			
(5,0) Non-optimized	**(5,0) CNT diameter optimized only**	**(6,0) Non-optimized**	**(7,0) Non-optimized**
0.0	0.0	0.0	0.0
2.5	5.5	6.3	0.0
48.4	19.8	123.7	327.5
58.7	26.7	123.8	327.5
78.2	96.0	143.1	613.9
81.8	97.4	144.5	613.9
172. 5	198.9	144.5	850.4
184.3	203.6	156.9	853.0
248.4	219.3	239.9	1032.6
581.6	411.0	240.0	1032.6
611.2	412.9	292.3	1145.7
622.3	418.4	295.4	1149.2
651.4	422.3	295.6	1187.2

Table S6. The *g* tensors of the lowest doublets of Tb^{3+} in (5,0), (6,0) and (7,0) CNTs (non-optimized) and (5,0) CNT (CNT diameter optimized only).

Doublets		**(5,0) Non-optimized**	**(5,0) CNT diameter optimized only**	**(6,0) Non-optimized**	**(7,0) Non-optimized**
1	g_X	0.0	0.0	0.0	0.0
	g_Y	0.0	0.0	0.0	0.0
	g_Z	17.4	15.6	17.2	17.9
2	g_X	0.0	0.0	0.0	0.0
	g_Y	0.0	0.0	0.0	0.0
	g_Z	15.8	15.1	0.5	14.6
3	g_X	0.0	0.0	0.0	0.0
	g_Y	0.0	0.0	0.0	0.0
	g_Z	16.8	17.7	0.1	11.4

4	g_X	0.0	0.0	0.0	0.0
	g_Y	0.0	0.0	0.0	0.0
	g_Z	9.9	12.1	11.7	8.4

Table S7. *Ab initio* results for the J=6 multiplet of Tb^{3+} in (5,0) CNT (non-optimized).

Spin-orbit singlets	E/cm^{-1}	Wavefunction
1	0.0	$95.0\%|\pm 6\rangle$
2	2.5	$99.8\%|\pm 6\rangle$
3	48.4	$39.4\%|\pm 1\rangle + 39.8\%|\pm 3\rangle + 20.8\%|\pm 5\rangle$
4	58.7	$18.6\%|0\rangle + 47.4\%|\pm 2\rangle + 29.0\%|\pm 4\rangle$
5	78.2	$42.6\%|\pm 1\rangle + 39.0\%|\pm 3\rangle + 18.4\%||\pm 5\rangle$
6	81.8	$22.1\%|0\rangle + 49.6\%|\pm 2\rangle + 28.4\%|\pm 4\rangle$
7	172.5	$16.8\%|\pm 3\rangle + 79.4\%|\pm 5\rangle$
8	184.3	$19.6\%|\pm 3\rangle + 76.6\%|\pm 5\rangle$
9	248.4	$99.8\%|\pm 4\rangle$
10	581.6	$58.5\%|0\rangle + 41.4\%|\pm 4\rangle$
11	611.2	$56.8\%|\pm 1\rangle + 40.6\%|\pm 3\rangle$
12	622.3	$53.6\%|\pm 1\rangle + 44.2\%|\pm 3\rangle$
13	651.4	$99.8\%|\pm 2\rangle$

Table S8. *Ab initio* results for the J=6 multiplet of Tb^{3+} in (5,0) CNT (CNT diameter optimized only).

Spin-orbit singlets	E/cm^{-1}	Wavefunction
1	0.0	$10.8\%|0\rangle + 10.0\%|\pm 2\rangle + 73.0\%|\pm 6\rangle$
2	5.5	$93.6\%|\pm 6\rangle$
3	19.8	$85.6\%|\pm 1\rangle + 13.2\%|\pm 3\rangle$
4	26.7	$38.3\%|0\rangle + 39.8\%|\pm 2\rangle + 20.8\%|\pm 6\rangle$
5	96.0	$77.0\%|\pm 1\rangle + 20.0\%|\pm 3\rangle$
6	97.4	$46.0\%|0\rangle + 48.0\%|\pm 2\rangle$
7	198.9	$12.0\%|\pm 1\rangle + 55.8\%|\pm 3\rangle + 27.4\%|\pm 5\rangle$
8	203.6	$85.2\%|\pm 2\rangle + 9.6\%|\pm 4\rangle$

9	219.3	20.2%$\lvert\pm 1\rangle$ + 46.4%$\lvert\pm 3\rangle$ + 31.4%$\lvert\pm 5\rangle$
10	411.0	9.2%$\lvert\pm 2\rangle$ + 6.0%$\lvert\pm 3\rangle$ + 75.2%$\lvert\pm 4\rangle$
11	412.9	81.6%$\lvert\pm 4\rangle$
12	418.4	23.0%$\lvert\pm 3\rangle$ + 9.2%$\lvert\pm 4\rangle$ + 64.0%$\lvert\pm 5\rangle$
13	422.3	27.4%$\lvert\pm 3\rangle$ + 63.4%$\lvert\pm 5\rangle$

Table S9. *Ab initio* results for the J= 6 multiplet of Tb^{3+} in (6,0) CNT (non-optimized).

Spin-orbit singlets	E/cm^{-1}	Wavefunction
1	0.0	95.2%$\lvert\pm 6\rangle$
2	6.3	100%$\lvert\pm 6\rangle$
3	123.7	79.8%$\lvert\pm 1\rangle$ + 20.2%$\lvert\pm 5\rangle$
4	123.8	79.6%$\lvert\pm 1\rangle$ + 20.4%$\lvert\pm 5\rangle$
5	143.1	95.0%$\lvert 0\rangle$
6	144.5	77.4%$\lvert\pm 2\rangle$ + 22.6%$\lvert\pm 4\rangle$
7	145.0	77.4%$\lvert\pm 2\rangle$ + 22.6%$\lvert\pm 4\rangle$
8	156.9	100%$\lvert\pm 3\rangle$
9	239.9	20.2%$\lvert\pm 1\rangle$ + 79.8%$\lvert\pm 5\rangle$
10	240.0	22.4%$\lvert\pm 1\rangle$ + 79.6%$\lvert\pm 5\rangle$
11	292.3	100%$\lvert\pm 3\rangle$
12	295.4	22.6%$\lvert\pm 2\rangle$ + 77.4%$\lvert\pm 4\rangle$
13	295.6	22.6%$\lvert\pm 2\rangle$ + 77.4%$\lvert\pm 4\rangle$

Table S10. *Ab initio* results for the J=6 multiplet of Tb^{3+} in (7,0) CNT (non-optimized).

Spin-orbit singlets	E/cm^{-1}	Wavefunction
1	0.0	100%$\lvert\pm 6\rangle$
2	0.0	100%$\lvert\pm 6\rangle$
3	327.5	100%$\lvert\pm 5\rangle$
4	327.5	100%$\lvert\pm 5\rangle$
5	613.9	100%$\lvert\pm 4\rangle$
6	613.9	100%$\lvert\pm 4\rangle$

7	850.4	100%$\vert \pm 3\rangle$
8	853.0	100%$\vert \pm 3\rangle$
9	1032.6	100%$\vert \pm 2\rangle$
10	1032.6	100%$\vert \pm 2\rangle$
11	1145.7	100%$\vert \pm 1\rangle$
12	1149.2	100%$\vert \pm 1\rangle$
13	1187.2	100%$\vert 0\rangle$

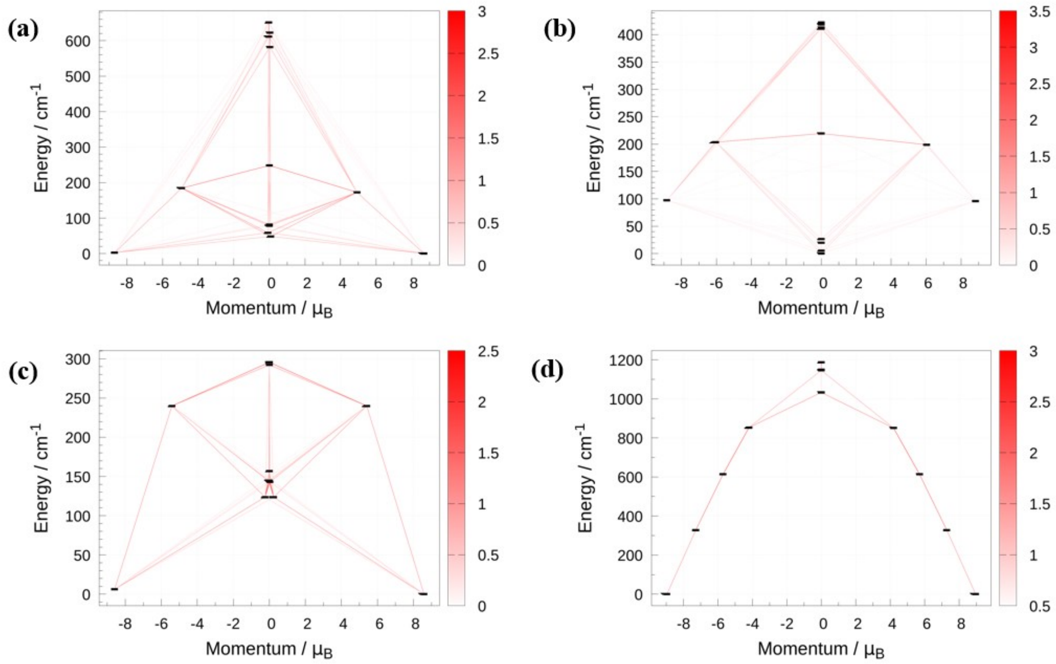

Figure S3. The relaxation paths for reversal of magnetization of Tb^{3+} in non-optimized (5,0), (6,0) and (7,0) CNTs [(a), (c), and (d), respectively] and for (5,0) CNT diameter optimized only (b).

Table S11. *Ab initio* results for the *J*=6 multiplet of Tb^{3+} in (5,0) CNT (fully optimized).

Spin-orbit singlets	***E*/cm^{-1}**	**Wavefunction**
1	0.0	99.0%$\vert \pm 6\rangle$
2	0.5	99.4%$\vert \pm 6\rangle$
3	82.0	8.8%$\vert \pm 3\rangle$ + 85.8%$\vert \pm 5\rangle$
4	89.5	96.4%$\vert \pm 5\rangle$
5	118.2	16.2%$\vert 0\rangle$ + 81.6%$\vert \pm 4\rangle$

6	144.7	30.0%$\vert\pm 2\rangle$ + 69.8%$\vert\pm 4\rangle$
7	155.1	31.4%$\vert\pm 1\rangle$ + 68.4%$\vert\pm 3\rangle$
8	188.4	13.4%$\vert\pm 1\rangle$ + 73.2%$\vert\pm 3\rangle$ + 13.2%$\vert\pm 5\rangle$
9	190.9	69.2%$\vert\pm 2\rangle$ + 29.4%$\vert\pm 4\rangle$
10	370.0	64.2%$\vert\pm 1\rangle$ + 30.2%$\vert\pm 3\rangle$
11	370.2	29.0%$\vert 0\rangle$ + 56.4%$\vert\pm 2\rangle$ + 12.0%$\vert\pm 4\rangle$
12	382.5	19.8%$\vert\pm 3\rangle$ + 81.2%$\vert\pm 1\rangle$
13	382.5	5.6%$\vert\pm 4\rangle$ + 53.8%$\vert 0\rangle$ + 40.2%$\vert\pm 2\rangle$

Table S12. *Ab initio* results for the *J*=6 multiplet of Tb^{3+} in (6,0) CNT (fully optimized).

Spin-orbit singlets	*E*/cm^{-1}	Wavefunction
1	0.0	94.6%$\vert\pm 6\rangle$
2	4.7	100%$\vert\pm 6\rangle$
3	85.9	88.2%$\vert\pm 1\rangle$ + 11.8%$\vert\pm 5\rangle$
4	87.4	87.6%$\vert\pm 1\rangle$ + 12.2%$\vert\pm 5\rangle$
5	95.3	92.8%$\vert 0\rangle$
6	102.2	82.6%$\vert\pm 2\rangle$ + 17.4%$\vert\pm 4\rangle$
7	103.7	81.6%$\vert\pm 2\rangle$ + 16.6%$\vert\pm 4\rangle$
8	114.7	99.8%$\vert\pm 3\rangle$
9	183.2	11.8%$\vert\pm 1\rangle$ + 88.0%$\vert\pm 5\rangle$
10	183.4	12.2%$\vert\pm 1\rangle$ + 87.8%$\vert\pm 5\rangle$
11	204.4	99.8%$\vert\pm 3\rangle$
12	213.6	16.8%$\vert\pm 2\rangle$ + 83.2%$\vert\pm 4\rangle$
13	214.6	17.4%$\vert\pm 2\rangle$ + 82.6%$\vert\pm 4\rangle$

Table S13. *Ab initio* results for the *J*=6 multiplet of Tb^{3+} in (7,0) CNT (fully optimized).

Spin-orbit singlets	*E*/cm^{-1}	Wavefunction
1	0.0	11.0%$\vert\pm 2\rangle$ + 19.4%$\vert\pm 4\rangle$ + 65.2%$\vert\pm 6\rangle$
2	15.1	13.8%$\vert\pm 4\rangle$ + 84.2%$\vert\pm 6\rangle$
3	49.0	31.2%$\vert\pm 1\rangle$ + 34.6%$\vert\pm 3\rangle$ + 34.4%$\vert\pm 5\rangle$

4	118.8	26.2%$\|\pm 3\rangle$ + 71.0%$\|\pm 5\rangle$
5	123.3	21.3%$\|0\rangle$ + 36.4%$\|\pm 2\rangle$ + 11.6%$\|\pm 4\rangle$ + 30.6%$\|$
6	265.4	24.2%$\|\pm 2\rangle$ + 51.2%$\|\pm 4\rangle$ + 13.6%$\|\pm 6\rangle$
7	269.3	33.8%$\|\pm 1\rangle$ + 52.4%$\|\pm 5\rangle$
8	484.9	13.6%$\|\pm 1\rangle$ + 49.6%$\|\pm 3\rangle$ + 7.8%$\|\pm 4\rangle$ + 25.0%
9	485.3	21.5%$\|0\rangle$ + 6.0%$\|\pm 1\rangle$ + 6.8%$\|\pm 3\rangle$ + 57.0%$\|\pm$
10	808.0	16.0%$\|\pm 1\rangle$ + 34.2%$\|\pm 2\rangle$ + 32.0%$\|\pm 3\rangle$ + 13.8
11	808.1	15.0%$\|\pm 1\rangle$ + 36.4%$\|\pm 2\rangle$ + 30.2%$\|\pm 3\rangle$ + 14.8
12	1477.5	21.9%$\|0\rangle$ + 46.0%$\|\pm 1\rangle$ + 20.0%$\|\pm 2\rangle$ + 9.8%$\|\pm$
13	1477.6	28.0%$\|0\rangle$ + 35.8%$\|\pm 1\rangle$ + 25.8%$\|\pm 2\rangle$ + 7.6%$\|\pm$

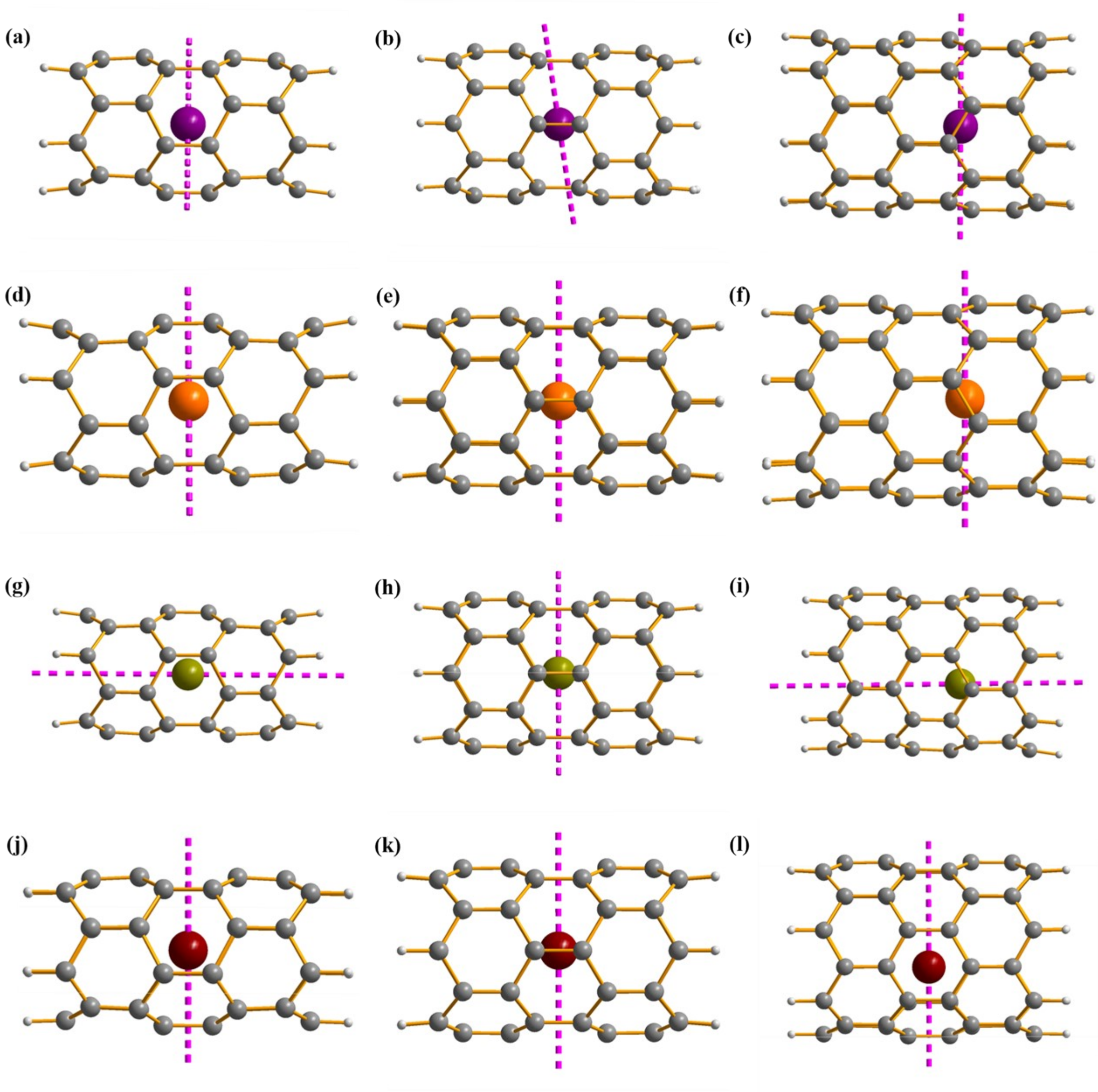

Figure S4. Structure of Ln^{3+} (Ln=Dy, Ho, Er and Tm top to bottom) in the (5,0), (6,0) and (7,0) CNT (left to right) and the main magnetic axis of the corresponding ground doublet (pink arrow). Color code: Dy^{3+} (violet), Ho^{3+} (orange), Er^{3+} (dark yellow), Tm^{3+} (dark red), H (gray) and C (dark gray).

Table S14. *Ab initio* results for the J=15/2 multiplet of Dy^{3+} in (5,0) CNT.

KDs	E/cm^{-1}	Wavefunction
1	0.0	$7.5\%\|\pm 3/2\rangle + 7.6\%\|\pm 7/2\rangle + 8.1\%\|\pm 9/2\rangle + 25.2\%\|\pm 13/2\rangle + 46.2\%\|\pm 15/2\rangle$
2	3.6	$10.0\%\|\pm 1/2\rangle + 8.9\%\|\pm 3/2\rangle + 16.7\%\|\pm 5/2\rangle + 19.7\%\|\pm 7/2\rangle + 17.5\%\|\pm 9/2\rangle + 11.7\%\|\pm 13/2\rangle + 11.8\%\|\pm 15/2\rangle$
3	85.5	$19.3\%\|\pm 1/2\rangle + 9.1\%\|\pm 5/2\rangle + 16.7\%\|\pm 7/2\rangle + 29.7\%\|\pm 9/2\rangle + 18.5\%\|\pm 11/2\rangle$
4	116.2	$18.3\%\|\pm 3/2\rangle + 38.3\%\|\pm 5/2\rangle + 26.4\%\|\pm 7/2\rangle + 16.1\%\|\pm 11/2\rangle$
5	143.4	$14.8\%\|\pm 1/2\rangle + 19.0\%\|\pm 3/2\rangle + 12.8\%\|\pm 9/2\rangle + 45.4\%\|\pm 11/2\rangle$
6	368.6	$15.6\%\|\pm 3/2\rangle + 23.0\%\|\pm 5/2\rangle + 13.2\% \pm 7/2\rangle + 20.2\%\|\pm 11/2\rangle + 9.8\%\|\pm 13/2\rangle$
7	425.0	$7.0\%\|\pm 1/2\rangle + 15.2\%\|\pm 9/2\rangle + 40.1\%\|\pm 13/2\rangle + 22.5\%\|\pm 15/2\rangle$
8	477.0	$41.7\%\|\pm 1/2\rangle + 22.9\%\|\pm 3/2\rangle + 10.4\%\|\pm 5/2\rangle + 10.1\%\|\pm 7/2\rangle$

Table S15. *Ab initio* results for the J=15/2 multiplet of Dy^{3+} in (6,0) CNT.

KDs	E/cm^{-1}	Wavefunction
1	0.0	$8.4\%\|\pm 1/2\rangle + 8.4\%\|\pm 5/2\rangle + 18.4\%\|\pm 9/2\rangle + 29.7\%\|\pm 11/2\rangle + 25.1\%\|\pm 13/2\rangle$
2	42.4	$11.7\%\|\pm 1/2\rangle + 17.0\%\|\pm 5/2\rangle + 29.3\%\|\pm 7/2\rangle + 20.8\%\|\pm 9/2\rangle + 14.6\%\|\pm 11/2\rangle$
3	49.6	$6.4\%\|\pm 9/2\rangle + 31.6\%\|\pm 11/2\rangle + 48.5\%\|\pm 13/2\rangle + 11.2\%\|\pm 15/2\rangle$
4	64.3	$6.4\%\|\pm 1/2\rangle + 20.8\%\|\pm 3/2\rangle + 23.1\%\|\pm 5/2\rangle + 21.9\%\|\pm 7/2\rangle + 22.6\%\|\pm 9/2\rangle$
5	272.4	$5.4\%\|\pm 1/2\rangle + 4.9\%\|\pm 5/2\rangle + 4.0\%\|\pm 7/2\rangle + 12.0\%\|\pm 13/2\rangle + 65.6\%\|\pm 15/2\rangle$
6	295.1	$38.0\%\|\pm 1/2\rangle + 35.0\%\|\pm 3/2\rangle + 7.1\%\|\pm 5/2\rangle + 6.7\%\|\pm 11/2\rangle + 6.9\%\|\pm 13/2\rangle$
7	338.3	$22.8\%\|\pm 1/2\rangle + 8.1\%\|\pm 3/2\rangle + 23.7\%\|\pm 5/2\rangle + 12.4\%\|\pm 7/2\rangle + 6.3\%\|\pm 11/2\rangle + 17.4\%\|\pm 15/2\rangle$

8	360.7	6.6%| ± 1/2⟩ + 22.5%| ± 3/2⟩ + 21.4%| ± 5/2⟩ + 27.5%| ± 7/2⟩ + 19.0%| ± 9/2⟩

Table S16. *Ab initio* results for the *J*=15/2 multiplet of Dy^{3+} in (7,0) CNT.

KDs	*E*/cm^{-1}	Wavefunction
1	0.0	6.1%| ± 7/2⟩ + 17.9%| ± 11/2⟩ + 69.9%| ± 15/2⟩
2	57.8	11.8%| ± 1/2⟩ + 6.8%| ± 3/2⟩ + 16.8%| ± 5/2⟩ + 23.7% ± 9/2⟩ + 30.6% ± 13/2⟩ + 7.7%| ± 15/2⟩
3	145.1	9.2%| ± 1/2⟩ + 17.9%| ± 3/2⟩ + 18.3%| ± 7/2⟩ + 6.9%| ± 11/2⟩ + 30.6% ± 13/2⟩ + 11.6%| ± 15/2⟩
4	302.7	12.3%| ± 1/2⟩ + 18.0%| ± 5/2⟩ + 11.4%| ± 7/2⟩ + 27.0%| ± 11/2⟩ + 20.6% ± 13/2⟩ + 7.6%| ± 15/2⟩
5	534.1	20.1% ± 3/2⟩ + 8.9%| ± 5/2⟩ + 22.7%| ± 9/2⟩ + 27.4%| ± 11/2⟩ + 12.4%| ± 13/2⟩
6	839.3	18.9%| ± 1/2⟩ + 5.0%| ± 5/2⟩ + 24.5% ± |7/2⟩ + 28.6%| ± 9/2⟩ + 15.5%| ± 11/2⟩
7	1162.0	18.9%| ± 3/2⟩ + 31.4%| ± 5/2⟩ + 27.2%| ± 7/2⟩ + 14.3%| ± 9/2⟩
8	1367.5	39.5%| ± 1/2⟩ + 30.7%| ± 3/2⟩ + 18.3%| ± 5/2⟩ + 8.2%| ± 7/2⟩

Table S17. *Ab initio* results for the *J*=8 multiplet of Ho^{3+} in (5,0) CNT.

Spin-orbit singlets	*E*/cm^{-1}	Wavefunction
1	0.0	17.4%| ± 6⟩ + 77.0%| ± 8⟩
2	0.5	17.2%| ± 6⟩ + 77.4%| ± 8⟩
3	85.8	10.4%| ± 2⟩ + 28.8%| ± 3⟩ + 23.2%| ± 4⟩ + 22.6%| ± 5⟩ 7.2%| ± 6⟩
4	85.8	14.4%| ± 2⟩ + 20.2%| ± 3⟩ + 32.6%| ± 4⟩ + 16.6%| ± 5⟩ 10.4%| ± 6⟩
5	117.0	11.2%| ± 1⟩ + 80.6%| ± 5⟩ + 7.0%| ± 7⟩
6	119.5	10.2%| ± 2⟩ + 67.4%| ± 4⟩ + 21.6%| ± 6⟩
7	121.9	26.6%| ± 3⟩ + 33.4%| ± 5⟩ + 36.8%| ± 7⟩
8	122.1	56.0%| ± 3⟩ + 8.6%| ± 5⟩ + 31.6%| ± 7⟩

9	163.2	27.7%|0⟩ + 44.6%| ± 2⟩ + 20.0%| ± 4⟩ + 6.2%| ± 8⟩
10	196.5	40.8%| ± 2⟩ + 25.0%| ± 4⟩ + 16.4%| ± 6⟩ + 14.8%| ± 8⟩
11	200.1	64.0%| ± 1⟩ + 29.2%| ± 7⟩
12	256.8	5.4%| ± 1⟩ + 25.4%| ± 3⟩ + 5.6%| ± 5⟩ + 10.6%| ± 6⟩ + 44.4%| ± 7⟩
13	257.2	9.6%|0⟩ + 9.6%| ± 4⟩ + 44.4%| ± 6⟩ + 10.8%| ± 7⟩ + 12.6%| ± 8⟩
14	292.5	15.0%| ± 1⟩ + 9.4%| ± 2⟩ + 26.8%| ± 3⟩ + 12.4%| ± 5⟩ + 8.6%| ± 6⟩ + 26.2%| ± 7⟩
15	292.9	37.4%| ± 2⟩ + 6.6%| ± 3⟩ + 35.4%| ± 6⟩ + 6.2%| ± 7⟩ + 6.0%| ± 8⟩
16	328.4	14.6%|0⟩ + 6.0%| ± 2⟩ + 62.8%| ± 1⟩ + 10.4%| ± 5⟩
17	328.4	44.2%|0⟩ + 20.6%| ± 1⟩ + 18.2%| ± 2⟩ + 6.0%| ± 4⟩ + 6.8%| ± 6⟩

Table S18. *Ab initio* results for the *J*=8 multiplet of Ho^{3+} in (6,0) CNT.

Spin-orbit singlets	*E*/cm^{-1}	Wavefunction
1	0.0	24.8%| ± 1⟩ + 6.6%| ± 3⟩ + 57.2%| ± 7⟩
2	15.3	7.2%| ± 3⟩ + 83.8%| ± 7⟩
3	17.1	33.7%|0⟩ + 24.6%| ± 2⟩ + 32.0%| ± 6⟩
4	76.0	50.6%| ± 1⟩ + 9.4%| ± 2⟩ + 8.0%| ± 6⟩ + 28.0%| ± 7⟩
5	76.5	5.8%| ± 2⟩ + 11.4%| ± 5⟩ + 61.8%| ± 7⟩ + 10.6%| ± 8⟩
6	142.4	23.7%|0⟩ + 8.6%| ± 5⟩ + 38.4%| ± 6⟩ + 9.8%| ± 8⟩
7	269.8	20.9%0⟩ + 44.4%| ± 1⟩ + 20.6%| ± 2⟩
8	270.1	16.6%|0⟩ + 31.4%| ± 1⟩ + 25.6%| ± 2⟩ + 15.0%| ± 3⟩ 8.8%| ± 4⟩
9	284.5	13.4%| ± 1⟩ + 17.0%| ± 3⟩ + 15.6%| ± 4⟩ + 37.4%| ± 5 6.6%| ± 6⟩
10	342.6	11.2%| ± 1⟩ + 14.8%| ± 3⟩ + 13.6%| ± 4⟩ + 49.4%| ± 5 5.8%| ± 6⟩
11	342.7	7.2%| ± 1⟩ + 57.8%| ± 2⟩ + 15.4%| ± 3⟩ + 11.0%| ± 4⟩ 6.6%| ± 8⟩
12	481.4	13.2%| ± 2⟩ + 33.8%| ± 4⟩ + 20.6%| ± 6⟩ + 25.6%| ± 8

13	501.6	7.4%| ± 2⟩ + 13.8%| ± 4⟩ + 17.8%| ± 6⟩ + 52.8%| ± 8⟩
14	502.6	6.2%| ± 2⟩ + 47.6%| ± 3⟩ + 38.8%| ± 5⟩
15	559.4	33.4%| ± 4⟩ + 5.0%| ± 5⟩ + 54.4%| ± 8⟩
16	559.7	8.4%| ± 2⟩ + 58.4%| ± 3⟩ + 26.8%| ± 5⟩
17	583.0	9.8%| ± 2⟩ + 49.2%| ± 4⟩ + 5.0%| ± 5⟩ + 29.4%| ± 8⟩

Table S19. *Ab initio* results for the *J*=8 multiplet of Ho^{3+} in (7,0) CNT.

Spin-orbit singlets	***E*/cm^{-1}**	**Wavefunction**
1	0.0	11.4%| ± 2⟩ + 16.0%| ± 4⟩ + 19.0%| ± 6⟩ + 47.0%| ±
2	21.0	8.0%| ± 4⟩ + 17.2%| ± 6⟩ + 71.0%| ± 8⟩
3	36.4	24.0%| ± 1⟩ + 28.6%| ± 3⟩ + 26.8%| ± 5⟩ + 18.4%| ± 7
4	101.6	17.2%| ± 3⟩ + 33.2%| ± 5⟩ + 34.8%| ± 7⟩
5	107.7	10.5%|0⟩ + 20.4%| ± 2⟩ + 14.4%| ± 4⟩ + 9.0%| ± 7⟩ + 40.2%| ± 8⟩
6	180.4	7.4%| ± 1⟩ + 10.6%| ± 2⟩ + 27.2%| ± 4⟩ + 17.4%| ± 6 14.8%| ± 7⟩ + 19.2%| ± 8⟩
7	249.4	21.6%| ± 1⟩ + 6.6%| ± 3⟩ + 8.0%| ± 4⟩ + 7.2%| ± 6⟩ + 44.0%| ± 7⟩ + 6.2%| ± 8⟩
8	317.3	18.4%| ± 3⟩ + 4.8%| ± 5⟩ + 20.2%| ± 6⟩ + 39.0%| ± 7⟩ 5.2%| ± 8⟩
9	321.6	15.2%|0⟩ + 12.2%| ± 2⟩ + 14.8%| ± 3⟩ + 5.0%| ± 5⟩ + 33.2%| ± 6⟩ + 10.2%| ± 7⟩
10	382.0	10.6%| ± 1⟩ + 23.4%| ± 2⟩ + 9.6%| ± 4⟩ + 13.2%| ± 5⟩ 33.4%| ± 6⟩ + 7.8%| ± 7⟩
11	390.1	17.0%| ± 1⟩ + 10.0%| ± 2⟩ + 33.4%| ± 5⟩ + 18.4%| ± 6 13.2%| ± 7⟩
12	423.7	17.5%|0⟩ + 5.8%| ± 3⟩ + 42.2%| ± 4⟩ + 11.2%| ± 5⟩ + 17.2%| ± 6⟩
13	426.4	15.8%| ± 1⟩ + 16.8%| ± 3⟩ + 9.8%| ± 4⟩ + 39.2%| ± 5⟩ 7.8%| ± 6⟩
14	478.1	49.0%| ± 2⟩ + 43.2%| ± 4⟩ + 5.8%| ± 6⟩
15	478.2	17.6%| ± 1⟩ + 57.8%| ± 3⟩ + 21.8%| ± 5⟩
16	671.8	69.8%| ± 1⟩ + 26.2%| ± 3⟩

17	672.0	39.3%|0⟩ + 48.4%| ± 2⟩ + 11.0%| ± 4⟩

Table S20. *Ab initio* results for the *J*=15/2 multiplet of Er^{3+} in (5,0) CNT.

KDs	*E*/cm^{-1}	Wavefunction
1	0.0	57.0%| ± 11/2⟩ + 40.6%| ± 15/2⟩
2	18.3	7.9%| ± 1/2⟩ + 83.6%| ± 9/2⟩ + 8.1%| ± 15/2⟩
3	51.8	97.5%| ± 7/2⟩
4	103.9	12.8%| ± 1/2⟩ + 8.1%| ± 3/2⟩ + 71.2%| ± 5/2⟩
5	154.1	18.2%| ± 1/2⟩ + 63.3%| ± 3/2⟩ + 17.5%| ± 5/2⟩
6	213.1	10.1%| ± 9/2⟩ + 89.1%| ± 13/2⟩
7	257.5	42.0%| ± 11/2⟩ + 57.9%| ± 15/2⟩
8	289.6	68.7%| ± 1/2⟩ + 28.3%| ± 3/2⟩

Table S21. *Ab initio* results for the *J*=15/2 multiplet of Er^{3+} in (6,0) CNT.

KDs	*E*/cm^{-1}	Wavefunction
1	0.0	63.1%| ± 1/2⟩ + 19.6%| ± 11/2⟩ + 17.3%| ± 13/2⟩
2	57.7	66.9%| ± 3/2⟩ + 29.9%| ± 9/2⟩
3	98.1	57.4%| ± 5/2⟩ + 42.6%| ± 7/2⟩
4	233.7	23.4%| ± 11/2⟩ + 73.4%| ± 13/2⟩
5	310.6	94.5%| ± 15/2⟩
6	432.	33.7%| ± 1/2⟩ + 56.9%| ± 11/2⟩ + 9.3%| ± 13/2⟩
7	529.50	32.7%| ± 3/2⟩ + 65.0%| ± 9/2⟩
8	579.6	42.6%| ± 5/2⟩ + 57.4%| ± 7/2⟩

Table S22. *Ab initio* results for the *J*=15/2 multiplet of Er^{3+} in (7,0) CNT.

KDs	*E*/cm^{-1}	Wavefunction
1	0.	99.4%| ± 15/2⟩
2	199.63	96.4%| ± 13/2⟩

3	246.2	91.5%$\lvert\pm 11/2\rangle$
4	284.3	90.5%$\lvert\pm 9/2\rangle$
5	346.8	11.1%$\lvert\pm 5/2\rangle$ + 84.9%$\lvert\pm 7/2\rangle$
6	481.1	85.8%$\lvert\pm 5/2\rangle$ + 11.0%$\lvert\pm 7/2\rangle$
7	571.5	7.8%$\lvert\pm 1/2\rangle$ + 85.2%$\lvert\pm 3/2\rangle$
8	646.7	85.9%$\lvert\pm 1/2\rangle$ + 8.4%$\lvert\pm 3/2\rangle$

Table S23. *Ab initio* results for the J=6 multiplet of Tm^{3+} in (5,0) CNT.

Spin-orbit singlets	E/cm^{-1}	Wavefunction
1	0.0	9.3%$\lvert 0\rangle$ + 8.6%$\lvert\pm 1\rangle$ + 21.4%$\lvert\pm 2\rangle$ + 17.0%$\lvert\pm 3\rangle$ + 9.0%$\lvert\pm 5\rangle$ + 32.2%$\lvert\pm 6\rangle$
2	88.9	4.8%$\lvert\pm 2\rangle$ + 4.0%$\lvert\pm 3\rangle$ + 17.0%$\lvert\pm 5\rangle$ + 71.2%$\lvert\pm 6\rangle$
3	104.0	55.2%$\lvert\pm 1\rangle$ + 21.0%$\lvert\pm 3\rangle$ + 16.4%$\lvert\pm 4\rangle$
4	145.7	30.9%$\lvert 0\rangle$ + 56.8%$\lvert\pm 2\rangle$ + 5.4%$\lvert\pm 4\rangle$
5	197.1	31.8%$\lvert\pm 1\rangle$ + 20.2%$\lvert\pm 3\rangle$ + 11.0%$\lvert\pm 5\rangle$ + 34.6%$\lvert\pm 6\rangle$
6	220.8	25.8%$\lvert 0\rangle$ + 39.2%$\lvert\pm 1\rangle$ + 15.6%$\lvert\pm 2\rangle$ + 14.4%$\lvert\pm 6\rangle$
7	379.5	22.6%$\lvert 0\rangle$ + 8.8%$\lvert\pm 1\rangle$ + 20.4%$\lvert\pm 3\rangle$ + 38.0%$\lvert\pm 4\rangle$
8	428.0	55.4%$\lvert\pm 2\rangle$ + 33.4%$\lvert\pm 3\rangle$ + 9.0%$\lvert\pm 5\rangle$
9	432.2	7.8%$\lvert\pm 3\rangle$ + 46.0%$\lvert\pm 4\rangle$ + 31.8%$\lvert\pm 5\rangle$ + 12.0%$\lvert\pm 6\rangle$
10	451.3	9.0%$\lvert\pm 1\rangle$ + 24.8%$\lvert\pm 3\rangle$ + 45.2%$\lvert\pm 4\rangle$ + 12.8%$\lvert\pm 5\rangle$
11	467.2	32.0%$\lvert\pm 1\rangle$ + 26.6%$\lvert\pm 2\rangle$ + 33.6%$\lvert\pm 3\rangle$ + 7.2%$\lvert\pm 6\rangle$
12	491.9	10.3%$\lvert 0\rangle$ + 13.6%$\lvert\pm 3\rangle$ + 58.2%$\lvert\pm 5\rangle$ + 11.0%$\lvert\pm 6\rangle$
13	493.0	9.4%$\lvert\pm 1\rangle$ + 10.2%$\lvert\pm 2\rangle$ + 33.6%$\lvert\pm 4\rangle$ + 39.8%$\lvert\pm 5\rangle$ + 7.0%$\lvert\pm 6\rangle$

Table S24. *Ab initio* results for the J=6 multiplet of Tm^{3+} in (6,0) CNT.

Spin-orbit singlets	E/cm^{-1}	Wavefunction
1	0.0	34.4%$\lvert\pm 1\rangle$ + 65.2%$\lvert\pm 5\rangle$
2	29.8	98.2%$\lvert\pm 5\rangle$
3	30.1	39.2%$\lvert 0\rangle$ + 29.4%$\lvert\pm 2\rangle$ + 9.4%$\lvert\pm 4\rangle$ + 21.8%$\lvert\pm 6\rangle$
4	75.2	43.9%$\lvert 0\rangle$ + 29.2%$\lvert\pm 4\rangle$ + 26.6%$\lvert\pm 6\rangle$

5	81.8	$8.2\%\lvert\pm 1\rangle + 33.0\%\lvert\pm 4\rangle + 53.0\%\lvert\pm 6\rangle$
6	85.0	$51.8\%\lvert\pm 1\rangle + 5.8\%\lvert\pm 3\rangle + 5.2\%\lvert\pm 4\rangle + 29.4\%\lvert\pm 5\rangle + 7.$
7	194.1	$76.6\%\lvert\pm 1\rangle + 21.6\%\lvert\pm 3\rangle$
8	255.3	$13.3\%\lvert 0\rangle + 68.0\%\lvert\pm 2\rangle + 17.6\%\lvert\pm 6\rangle$
9	319.4	$30.6\%\lvert\pm 2\rangle + 47.6\%\lvert\pm 4\rangle + 21.6\%\lvert\pm 6\rangle$
10	353.6	$7.2\%\lvert\pm 3\rangle + 55.4\%\lvert\pm 4\rangle + 30.2\%\lvert\pm 6\rangle$
11	3549	$20.4\%\lvert\pm 1\rangle + 69.8\%\lvert\pm 3\rangle + 5.2\%\lvert\pm 4\rangle$
12	400.3	$16.4\%\lvert\pm 2\rangle + 72.2\%\lvert\pm 3\rangle$
13	400.3	$51.4\%\lvert\pm 2\rangle + 21.2\%\lvert\pm 3\rangle + 10.4\%\lvert\pm 4\rangle + 15.0\%\lvert\pm 6\rangle$

Table S25. *Ab initio* results for the J=6 multiplet of Tm^{3+} in (7,0) CNT.

Spin-orbit singlets	E/cm^{-1}	Wavefunction
1	0.0	$8.0\%\lvert\pm 4\rangle + 87.0\%\lvert\pm 6\rangle$
2	4.0	$91.0\%\lvert\pm 6\rangle$
3	57.3	$10.2\%\lvert\pm 2\rangle + 20.4\%\lvert\pm 3\rangle + 20.0\%\lvert\pm 4\rangle + 41.6\%\lvert\pm 5\rangle$
4	64.5	$8.2\%\lvert\pm 1\rangle + 22.6\%\lvert\pm 3\rangle + 19.0\%\lvert\pm 4\rangle + 40.8\%\lvert\pm 5\rangle$
5	176.6	$18.9\%\lvert 0\rangle + 33.8\%\lvert\pm 2\rangle + 20.6\%\lvert\pm 3\rangle + 9.4\%\lvert\pm 4\rangle + 8.$
6	185.3	$33.6\%\lvert\pm 1\rangle + 24.6\%\lvert\pm 2\rangle + 15.6\%\lvert\pm 3\rangle + 25.2\%\lvert\pm 4\rangle$
7	301.3	$24.0\%\lvert\pm 1\rangle + 7.2\%\lvert\pm 2\rangle + 12.2\%\lvert\pm 4\rangle + 49.4\%\lvert\pm 5\rangle$
8	384.3	$6.4\%\lvert\pm 1\rangle + 27.2\%\lvert\pm 3\rangle + 13.0\%\lvert\pm 4\rangle + 47.0\%\lvert\pm 5\rangle$
9	392.7	$24.2\%\lvert 0\rangle + 10.4\%\lvert\pm 2\rangle + 13.4\%\lvert\pm 3\rangle + 46.6\%\lvert\pm 4\rangle$
10	559.8	$28.2\%\lvert\pm 1\rangle + 58.4\%\lvert\pm 3\rangle + 7.8\%\lvert\pm 5\rangle$
11	567.7	$59.6\%\lvert\pm 2\rangle + 32.8\%\lvert\pm 4\rangle$
12	721.9	$38.5\%\lvert 0\rangle + 17.4\%\lvert\pm 1\rangle + 36.8\%\lvert\pm 2\rangle$
13	725.9	$12.7\%\lvert 0\rangle + 64.2\%\lvert\pm 1\rangle + 7.4\%\lvert\pm 2\rangle + 13.2\%\lvert\pm 3\rangle$

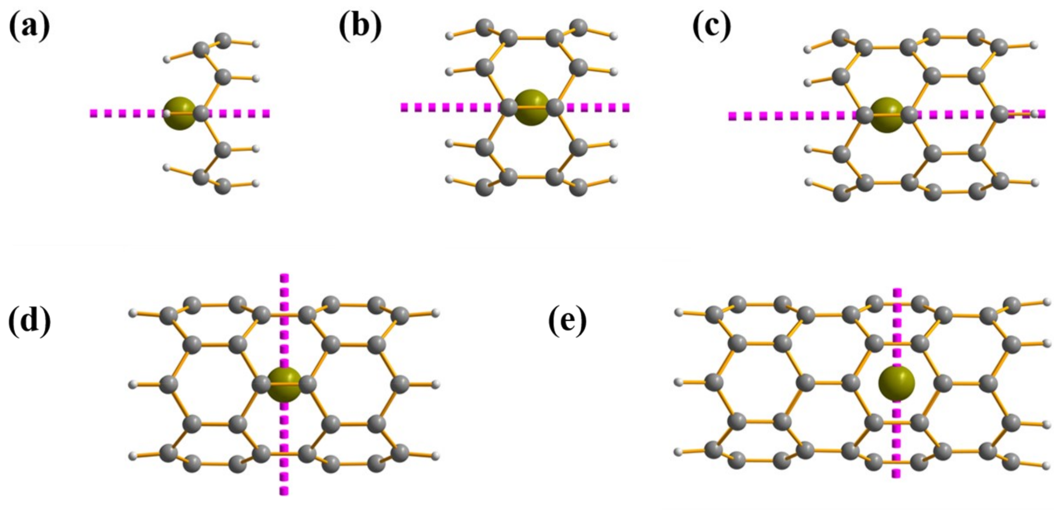

Figure S5. Fully optimized structure of Er^{3+} in (6,0) CNT of variable length of 1-5 stripes of carbon rings (a-e, respectively). Main magnetic axes are shown by pink dashed lines. Color code: Er^{3+} (dark yellow), H (gray) and C (dark gray).

Table S26. Energies of the lowest KDs for fully optimized structure of Er^{3+} in (6,0) CNT of variable length (1-5 stripes of carbon rings).

Spin-orbit energies, cm^{-1}				
1	**2**	**3**	**4**	**5**
0.0	0.0	0.0	0.0	0.0
20.6	69.6	50.2	57.7	57.8
95.4	174.6	83.4	98.1	95.7
114.6	263.1	200.0	233.7	215.7
151.7	325.6	279.9	310.5	283.5
727.7	452.9	378.6	432.8	426.6
763.5	619.0	464.3	529.5	524.5
796.0	721.3	510.4	579.6	577.9

Table S27. The *g* factors of the lowest KDs for fully optimized structure of Er^{3+} in (6,0) CNT of variable length (1-5 stripes of carbon rings).

KDs		**1**	**2**	**3**	**4**	**5**
1	g_X	0.1	3.0	4.1	8.4	8.3
	g_Y	0.2	3.0	4.1	8.4	8.3
	g_Z	14.5	13.2	11.8	0.9	1.1

2	g_X	7.0	0.0	0.0	0.2	0.1
	g_Y	6.6	0.0	0.0	0.2	0.1
	g_Z	4.5	17.3	16.8	0.2	0.3
3	g_X	9.2	0.7	1.9	9.0	8.9
	g_Y	8.5	0.7	1.9	8.6	8.7
	g_Z	2.0	6.2	5.0	0.1	0.2
4	g_X	0.3	0.0	0.0	4.9	5.0
	g_Y	0.4	0.0	0.1	5.0	5.1
	g_Z	2.9	1.6	1.6	8.4	7.8

Table S28. Energies of the *J*=7/2 KDs of Yb^{3+} in (5,0) CNT.

Spin-orbit energies, cm^{-1}
0.0
32.0
256.2
303.8

Table S29. The *g* factors of the *J*=7/2 KDs of Yb^{3+} in (5,0) CNT.

KDs		***g***
1	g_X	1. 6
	g_Y	1. 7
	g_Z	6.7
2	g_X	0.1
	g_Y	0.6
	g_Z	7.2
3	g_X	3.6
	g_Y	3.5
	g_Z	1.5
4	g_X	0.7
	g_Y	0.8
	g_Z	7.5

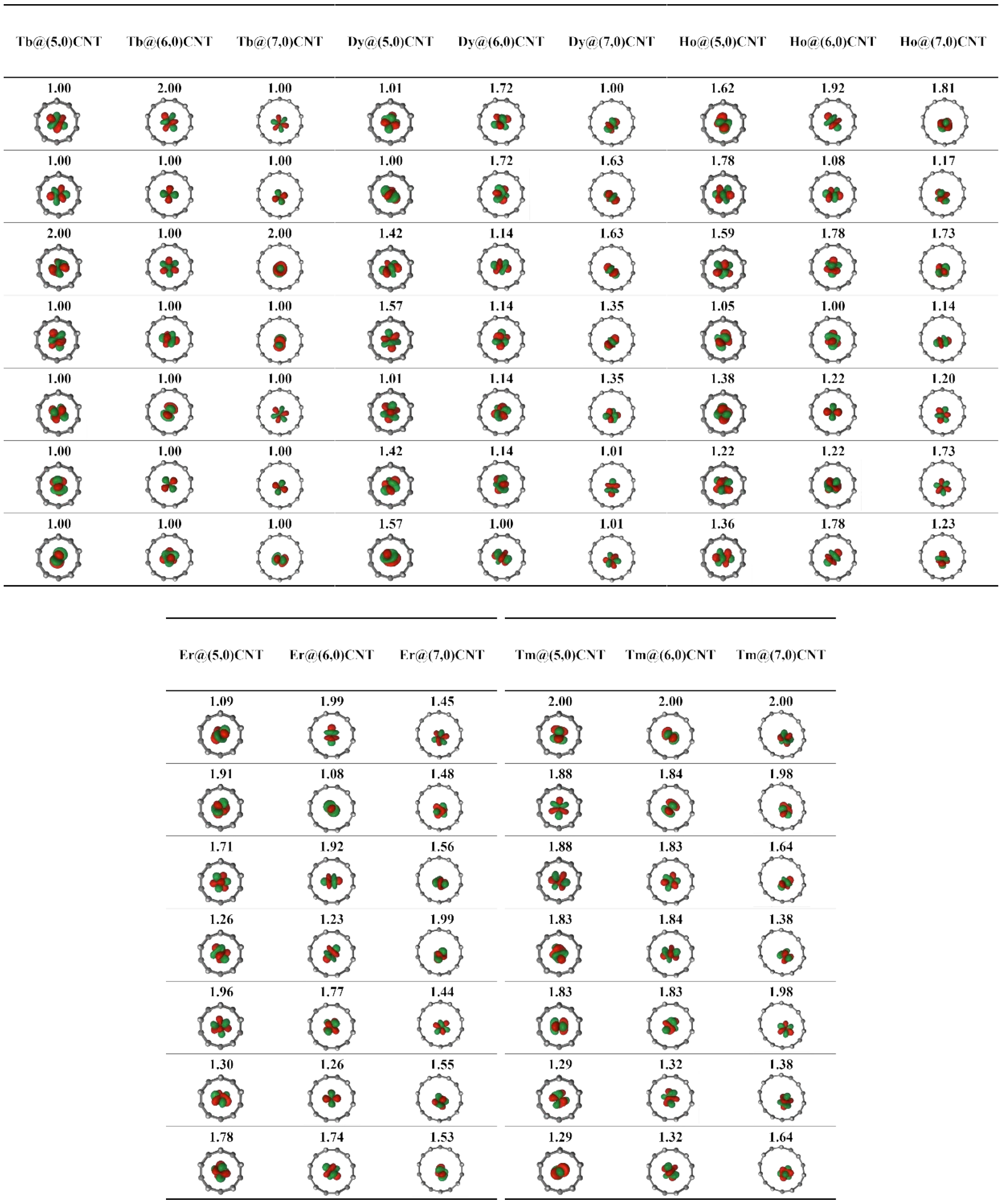

Figure S6 . The seven active molecular orbitals of 4*f* type for Ln^{3+}@CNT (Ln= Tb, Dy, Ho, Er and Tm) obtained in CASSCF/RASSI-SO. The isosurface corresponds to a value of 0.04. The number at each plot is the occupation number of the corresponding natural orbital in the ground state.

[1] A. Eatemadi *et al.*, Nanoscale Research Letters **9**, 393 (2014)